UNCLASSIFIED
SECURITY CLASSIFICATION OF THIS PAGE

(2)

REPORT DOCUMENTATION PAGE

DTIC ELECTE B 15 1988 H

DTIC FILE COPY

1a. REPORT SECURITY CLASSIFICATION: Unclassified	1b. RESTRICTIVE MARKINGS
AD-A205 029	3. DISTRIBUTION/AVAILABILITY OF REPORT: Approved for public release; distribution unlimited.
	5. MONITORING ORGANIZATION REPORT NUMBER(S): ARO 23394.3-EG
6a. NAME OF PERFORMING ORGANIZATION: Naval Postgraduate School	6b. OFFICE SYMBOL (If applicable): Code 67
7a. NAME OF MONITORING ORGANIZATION: U. S. Army Research Office	
6c. ADDRESS (City, State, and ZIP Code): Navy-NASA Joint Institute of Aeronautics, Dept. of Aeronautics & Astronautics, Naval Postgraduate School, Monterey, CA 93943	7b. ADDRESS (City, State, and ZIP Code): P. O. Box 12211, Research Triangle Park, NC 27709-2211
8a. NAME OF FUNDING/SPONSORING ORGANIZATION: U. S. Army Research Office	8b. OFFICE SYMBOL (If applicable)
9. PROCUREMENT INSTRUMENT IDENTIFICATION NUMBER	
8c. ADDRESS (City, State, and ZIP Code): P. O. Box 12211, Research Triangle Park, NC 27709-2211	10. SOURCE OF FUNDING NUMBERS: PROGRAM ELEMENT NO. / PROJECT NO. / TASK NO. / WORK UNIT ACCESSION NO.

11. TITLE (Include Security Classification)
Flow Visualization Studies of the Mach Number Effects on the Dynamic Stall of an Oscillating Airfoil.

12. PERSONAL AUTHOR(S) Chandrasekhara, M. S.
Carr, L. W., Aeroflightdynamics Directorate, U.S. Army ARTA

13a. TYPE OF REPORT	13b. TIME COVERED FROM ____ TO ____	14. DATE OF REPORT (Year, Month, Day)	15. PAGE COUNT
~~Reprint~~			

16. SUPPLEMENTARY NOTATION
The view, opinions and/or findings contained in this report are those of the author(s) and should not be construed as an official Department of the Army position, policy, or decision, unless so designated by other documentation.

17. COSATI CODES			18. SUBJECT TERMS (Continue on reverse if necessary and identify by block number)
FIELD	GROUP	SUB-GROUP	

19. ABSTRACT (Continue on reverse if necessary and identify by block number)

Compressibility effects on the dynamic stall of a NACA 0012 airfoil undergoing sinusoidal oscillatory motion were studied using a stroboscopic schlieren system. Schlieren pictures and some quantitative data derived from them are presented and show the influence of free-stream Mach number and reduced frequency on the dynamic-stall vortex. This study shows that a dynamic stall vortex always forms near the leading edge and convects on the airfoil upper surface at approximately 0.3 times the free stream velocity for all cases studied. The results also demonstrate that initiation of the dynamic stall vortex is delayed to higher angles of attack with increased reduced frequency, but that dynamic stall occurs at lower angles of incidence with increasing Mach numbers. (ede)

20 DISTRIBUTION/AVAILABILITY OF ABSTRACT	21. ABSTRACT SECURITY CLASSIFICATION
☐ UNCLASSIFIED/UNLIMITED ☐ SAME AS RPT. ☐ DTIC USERS	Unclassified
22a NAME OF RESPONSIBLE INDIVIDUAL	22b. TELEPHONE (Include Area Code) / 22c. OFFICE SYMBOL

DD FORM 1473, 84 MAR — 83 APR edition may be used until exhausted. All other editions are obsolete.

SECURITY CLASSIFICATION OF THIS PAGE
UNCLASSIFIED

AIAA '89

AIAA 89-0023
Flow Visualization Studies of the Mach Number Effects on the Dynamic Stall of an Oscillating Airfoil

M. Chandrasekhara, Naval Postgraduate School, Monterey, CA;
L. Carr, NASA-Ames, Moffett Field, CA

27th Aerospace Sciences Meeting
January 9–12, 1989/Reno, Nevada

AIAA-89-0023

FLOW VISUALIZATION STUDIES OF THE MACH NUMBER EFFECTS ON THE DYNAMIC STALL OF AN OSCILLATING AIRFOIL

M.S.Chandrasekhara[1]
Navy - NASA Joint Institute of Aeronautics
Naval Postgraduate School, Monterey, CA

and

L.W.Carr[2]
Aeroflightdynamics Directorate, U.S. Army ARTA, and
Fluid Dynamics Research Branch, NASA
NASA Ames Research Center, Moffett Field, CA

Abstract

Compressibility effects on the dynamic stall of a NACA 0012 airfoil undergoing sinusoidal oscillatory motion were studied using a stroboscopic schlieren system. Schlieren pictures and some quantitative data derived from them are presented and show the influence of free-stream Mach number and reduced frequency on the dynamic-stall vortex. This study shows that a dynamic stall vortex *always* forms near the leading edge and convects on the airfoil upper surface at approximately 0.3 times the free stream velocity for all cases studied. The results also demonstrate that initiation of the the dynamic stall vortex is delayed to higher angles of attack with increased reduced frequency, but that dynamic stall occurs at lower angles of incidence with increasing Mach numbers.

Nomenclature

c	airfoil chord
f	frequency of oscillation, Hz
M	free stream Mach number
U_∞	free stream velocity
U_{DSV}	dynamic stall vortex convection velocity
X	chordwise distance
α	angle of attack
α_0	mean angle of attack
α_m	amplitude of oscillation
κ	reduced frequency = $\frac{\pi fc}{U_\infty}$
ω	circular frequency, radians/sec

[1] Assistant Director and Adjunct Research Professor, Sr. Member AIAA

[2] Research Scientist, Member AIAA

1.Introduction

Dynamic stall and unsteady lift have been the subject of considerable research over the past 15 years. Its application in the helicopter field - called the "retreating blade problem" - has led to many detailed investigations. For comprehensive reviews of the problem, the reader is referred to Carr [1] and McCroskey [2]. Basically, the phenomenon can be explained as follows: The flow past an airfoil remains attached for angles of attack much greater than the static stall angle when the airfoil is pitched rapidly past the static stall angle.This results in additional lift, which gets further enhanced by the formation of the dynamic stall vortex. The airfoil continues to produce lift well beyond the static stall angle as long as the vortex remains on the surface of the airfoil. Thus, unsteady motion has also become a very attractive approach to increase the lift on fixed wing aircraft[3].

However, to exploit the benefits of this phenomenon in practice, a better understanding of the formation and behavior of the dynamic stall vortex at flight speeds is needed. McCroskey et al.[4] have indicated that the character of the dynamic stall process changes when the free stream Mach number exceeds about 0.2 since the maximum speed near the leading edge reaches sonic velocity, even at these low free stream velocities. As the Mach number increases beyond this value, the local flow around the leading edge can become supersonic , as can be seen from figure 1[4]. When supersonic velocities occur over an airfoil in steady flow, a shock usually forms; if a shock appears in the unsteady flow it could dramatically affect the dynamic stall process. Although there has been no direct experimental evidence to substantiate the presence of the shock on a dynamically stalling

airfoil, calculations by Fung and Carr [5] indicate its presence near the location of peak suction pressure. It has also been experimentally determined that trailing edge stall changes to leading edge stall as the Mach number increases from 0.2 to 0.3[4]. In fact, there is evidence that compressibility effects may even negate the benefits of dynamic stall[6].

This brief review of previous work shows that compressibility effects are potentially very important and need better understanding. In particular, the key to understanding the dynamic stall process lies in understanding the flow physics near the leading edge. One of the first steps toward this goal is to produce high quality flow visualization. Since the velocities are high and the flow is largely separated and turbulent, most methods of flow visualization will not work satisfactorily. The research to be presented in this paper reflects a new and novel approach to obtaining this important experimental information. The paper describes the dynamic stall process using a stroboscopic schlieren method which documents the vortex growth during its various stages of development for a range of Mach numbers and reduced frequencies. Resulting analysis of the images shows that compressibility has a direct impact on dynamic stall.

2. Description of the Facility, Instrumentation and Technique

The experiments were conducted in the newly built *Compressible Dynamic Stall Facility (CDSF)* in the Fluid Mechanics Laboratory (FML) of the NASA Ames Research Center. The CDSF is an in-draft wind tunnel with a 25 cm X 35 cm test section, driven by the FML compressor, which is connected to the tunnel exit throat (for details see Carr and Chandrasekhara[7]). The compressor maintains a vacuum pressure sufficient to create sonic velocity at the throat which is located downstream of the test section. The tunnel velocity is controlled by varying the area of this throat.

The uniqueness of the CDSF is that it has been specifically designed for dynamic stall flow visualization studies at high speeds. Unobstructed viewing of the complete flow field sorrounding the airfoil during unsteady motion is possible in the facility. This allows unobstructed quantitative as well as qualitative non-intrusive diagnosis (including laser Doppler velocimetry and holographic interferometry) of the instantaneous unsteady flow conditions that occur during dynamic stall. To achieve this, the airfoil is simply-supported by pins between two 2.54cm thick optical quality glass windows. The pins are smaller than the local airfoil thickness so that there is no obstruction of the airfoil contour by the support mechanism. The window/airfoil combination is driven in sinusoidal oscillation by a 4-bar, push-rod-flywheel system, about the 25% chord point as shown in figure 2. The drive motor is a variable speed a.c. motor with a controller to maintain speed to within 1%. The clearance between the airfoil and the window is about 0.5mm. A thin circular rubber cushion separates the glass windows from the airfoil, to prevent the danger of breaking the windows due to impact of the airfoil should any lateral movement occur during oscillation. The airfoil model is pinned at 25% and 70% chord.

Three encoders are used to register the mean angle of attack, the instantaneous amplitude of oscillation, and the phase angle/frequency information. The drive mechanism can oscillate the airfoil at frequencies of up to 100 Hz, with oscillatory amplitudes ranging from $2^\circ - 10^\circ$. The mean angle of attack can be varied from $0^\circ - 15^\circ$.

Flow visualization was obtained using a stroboscopic schlieren system. (see Fig.3). A Xenon arc lamp (EG&G, Inc. Model no. 1P-1, 1 mm arc length) is used as the light source; an iris diaphragm set at 0.5mm is located in front of the light source and serves to form a point source. The aperture is located at the focal point of a 45 cm. diameter, 3 m focal length concave mirror used to produce a parallel cylinder of light, which after passing through the test section is focussed by another concave mirror onto a vertical knife edge. The light that passes the knife edge is focussed by a lens and directed to the photographic focal plane a by plane mirror.

The strobe is triggered electronically at appropriate phase angles with custom built hardware using the output of the phase angle encoder. The light source can be pulsed either once for freeze action studies or any number of times for movies. In addition, this circuit can also be controlled by a computer. The circuit recycles rapidly and can trigger the strobe light at the highest frequency of interest (100 Hz). In practice, the phase angle was selected from the front panel switches. The actual phase angle at which the strobe was pulsed was displayed on the panel to serve as a check on the operation of the circuit. The flash duration was about 1.5 μsec.

The experiment consisted of taking single exposure photographs on Polaroid Type 52 film at the desired phase angle, for the matrix of test conditions presented in Table 1. In each run, the presence of the dynamic stall vortex was determined visually and pictures were taken at close phase intervals to study the dynamic stall development. Additional pictures were taken throughout the complete cycle.

2.1. Test conditions

The range of Mach number and reduced fre-

quency was chosen to encompass the conditions that occur on the retreating blade of helicopter rotors in forward flight. The specific tests were performed at the conditions shown in Table 1. (* indicates future tests planned). The experimental conditions were: $0.15 \leq M \leq 0.45$, $0 \leq \kappa \leq 0.1$, with the angle of attack $\alpha = \alpha_o - \alpha_m sin\omega t$, with $\alpha_o = \alpha_m = 10°$. The airfoil was NACA 0012, with 7.5 cm chord.

3. Results and Discussion

In this section, schlieren photographs are presented at selected angles as the airfoil undergoes a cycle of oscillation. A discussion of these photographs is followed by discussion of the effects of Mach number and reduced frequency and an evaluation of the convection velocity of the dynamic stall vortex. Some ideas on the control of the dynamic stall process are also offered.

3.1. Stroboscopic schlieren studies

Unlike other flow visualization methods that show the streamline or streakline patterns that integrate the past history of the flow, the schlieren technique enables instantaneous visualization of the flow. Each picture is a "snap shot" of the flow at the instant the photograph is taken, and shows the influence of the vortex on the flow field only at that time. Most published schlieren data are for flows with very strong density gradients such as shock waves which are highly visible. In the present experiment, the system was intentionally set to be very sensitive so that weak gradients could be made visible. It was possible to photograph the density gradient in the separated flow past a stationary airfoil at M = 0.1 with this system. It should be noted that, except near the leading edge, the density gradients are very small in the range of Mach numbers for which the experiments were conducted; even so the dynamic stall vortex is clearly visible.

Some notes of caution are appropriate: at certain phase angles, the leading edge of the airfoil appears to be in its own shadow and a ghost image can be seen in some photographs. The exact cause of this is not yet known; but it is suspected to be due to a slight misalignment of the system at some window angles, because it appears at the same angles for all flow cases studied and is independent of the flow. Also, the thin streaks which appear perpendicular to the airfoil on the upper and lower surfaces at 70% chord are due to cracks in the glass that appeared when the airfoil pins were being push-fitted into matching holes in the glass windows. Fortunately, the cracks did not propagate during the experiments. A new window is being fabricated and future tests will be free of this imperfection.

Schlieren photographs for several test conditions are presented in Fig. 4. They show the flow gradients at selected angles of attack for M = 0.3 and 0.4, for a fixed reduced frequency of 0.05. As can be seen from Fig. 4a, (M = 0.3) and 4b (M = 0.4), dynamic stall occurs at lower angles of attack for higher Mach numbers. At M = 0.3, the stall angle of attack is 15.9° and at M = 0.4, it is 14.5°. Conversely, at an angle of attack of 14.5° while the dynamic stall vortex remains on the surface and has progressed only to about 70% of the chord at M = 0.3, it has already been shed into the wake at M = 0.4.

Fig. 5 presents flow visualization pictures through a half cycle of oscillation consisting of pitch up from a mean angle of 10° to the maximum amplitude of 20° and then pitch down to 10° for M = 0.2 (Fig. 5a) and M = 0.3 (Fig. 5b) for $\kappa = 0.1$. The approximate location of the vortex core compares very well for both cases, establishing the independence of the process of dynamic stall formation up to M = 0.3.

The following observations can be made from the series of photographs in Fig. 5.

1. The dark region around the leading edge on the lower surface is the density field associated with the stagnation region. Its size and location changes with the angle of attack.

2. The flow accelerates near the leading edge (the white patch above the upper surface) and this region terminates in another dark region where the adverse pressure gradient results in positive density gradient. The dark region appears at lower values of angles of attack as the Mach number is increased. In this region, significant vorticity introduced by the pitching motion of the airfoil is present.

3. The vorticity in the dark region coalesces in the first 20% of the chord and becomes the dynamic stall vortex. Unfortunately, its exact origin is hard to separate from the density variations produced by the decelerating flow on the airfoil. The location at which this process is complete (and the vortex begins to move over the surface) depends on the Mach number and reduced frequency. This location occurs further downstream with increasing Mach number and further upstream with increasing reduced frequency. During the coalescence process, the vorticity generated near the leading edge is consolidated and the dynamic stall vortex fully forms at about 20% chord. It should be noted that by the time the stall vortex is fully formed, there is no additional (useful) vorticity input to the flow. The airfoil experiences leading edge stall, which can be seen clearly in the schlieren pictures as a white streak that originates at the leading edge. The vorticity that is generated is due to the extremely rapid accelerations generated here (see Reynolds and Carr [8]) and thus is indirectly due to pressure gradients. Once leading edge separation occurs this effect is lost. Considerable thickening of the

boundary layer occurs by the time the vortex has fully formed. This phenomenon is nearly the same at all Mach numbers and reduced frequencies.

4. As the airfoil continues to pitch up towards its maximum amplitude (20°), the dynamic stall vortex begins to convect downstream and eventually lifts off the surface and is shed into the wake. The angle at which the vortex is *released* from the surface or is convected past the trailing edge is strongly dependent upon the Mach number and reduced frequency (summarized in Table 2). As the Mach number is increased, dynamic stall is initiated at lower angles attack. As the reduced frequency is increased, the vortex remains on the upper surface until reaching higher angles of attack. Since earlier studies have pointed out that the airfoil generates lift as long as the vortex remains on the surface Carr et al[9], a form of dynamic stall control becomes available by simply increasing the oscillation frequency. All these angles are considerably higher than the static stall angles at the corresponding Mach numbers.

After the vortex has convected past the trailing edge, i.e. when the airfoil is experiencing deep stall, a vorticity layer can still be seen to separate the outer potential flow from the inner viscous layer.

5. During the downward motion of the airfoil, the flow starts to reattach at about 10° and the reattachment is complete between angles of attack 11° and 9°. Reattachment appears to be only a weak function of the parameters of this experiment.

6. At angles of incidence below 10° (or reattachment angle), no significant unsteady effects are present.

7. In many instances, trailing edge vortices and vortices in the separated shear layer can be identified. However, these do not appear to have any effect on the dynamic stall vortex or the process of its formation and passage down the airfoil surface.

8. No shocks could be identified in any of the conditions studied to date. However, the present schlieren system has been set up to visualize the global flow field and does not focus on the leading edge with sufficient detail to document the presence or absence of a shock whose dimensions, if present, are very small (suspected to be about 1 mm high and located between 0 - 5% chord). Also, the spanwise averaging effect of the schlieren technique may smear it. Future investigations will concentrate on this area.

3.2. Quantitative effects of compressibility

Although no shocks have been documented, the effects of compressibility are clearly shown in Fig. 6, in which pictures of the dynamic stall vortex at about 50% chord location are presented for M = 0.1, 0.2, 0.25, 0.35, 0.40 and 0.45. The angle of attack for a fixed vortex location remains constant till M = 0.3. This behavior indicates that stall occured earlier in the cycle at higher Mach numbers.

The location of the dynamic stall vortex, measured from the schlieren photographs are plotted in Fig. 7 at different points in the cycle, for different Mach numbers for κ = 0.05. The most striking feature is that up to M = 0.25, the vortex locations are nearly identical. For $M \geq 0.25$, rapid departures appear and with increasing Mach number, the stall vortex begins to appear at dramatically lower phase angles (angles of attack). M = 0.25 - 0.3 seems to be the demarkation between subcritical and supercritical flow over the airfoil. Thus compressibility plays a major role in the process of dynamic stall, causing it to occur at lower angles of attack.

In the present experiments, the Reynolds number was increased by a factor of 3 during the tests for M = 0.1 - 0.3. The Reynolds number ranged from 200,000 - 900,000. This did not affect the formation or the convection of the dynamic stall vortex as can be seen from Fig. 7. However, the figure also shows that a marked departure in the loci of the vortex locations appears for M $\geq$ 0.3. Thus, the trend seen is very clearly due to compressibility effects only.

Another interesting feature can also be seen from Figure 7. Once again, beginning at M = 0.3, departures in the inception and development of the dynamic stall vortex occur, and the point of inception moves further downstream from the leading edge with increasing Mach number. The reason for this is not clear at this time. It is theorised that the local supersonic flow plays an important role in the process of vortex formation, which includes the assimilation of the vorticity into the vortex. But, the vortex does indeed form at all Mach numbers. However, it appears that the vortex is weaker at higher Mach numbers, as evidenced by it being convected past the trailing edge at much lower angles of attack. The following heuristic reasoning may be offered for this: the flow separates at a lower angle of attack, and at this condition, the radius of curvature of the streamlines near the leading edge is smaller and hence the pressure gradient is reduced. Thus, the net vorticity introduced is smaller, which leads to the conclusion that the vortex is weaker.

3.3. Quantitative effects of reduced frequency

As mentioned earlier, the effect of increasing the reduced frequency is to keep the dynamic stall vortex on the surface to higher angles of attack. This can be seen more clearly in Fig. 8 for Mach numbers ranging from 0.25 to 0.45. In fact for κ = 0.1 and M = 0.20, the vortex remains on the surface for angles as high as 18.1°. Thus, a form of dynamic stall control

is evident by this result.The monotonic nature of its dependence on reduced frequency suggests that this method of control should work at all Mach numbers.

Once again, M = 0.3 is the free stream condition when compressibility effects appear. Of most interest is the appearance of the dynamic stall vortex (or at least, its impression on the schlieren) closer to the leading edge as the reduced frequency is increased. As can be seen from the figure, the location of the appearance of the dynamic stall vortex is independent of the reduced frequency in incompressible flow. The exact mechanism of the creation of the vortex is still not known. Its understanding will require a careful study of the events near the leading edge, which are being planned. But, it is hoped that the following ideas will be of some use in this context. The discussions presented by Reynolds and Carr [8] explain how the motion of the body causes significant vorticity to be input into the flow, depending on the pressure gradient created near the leading edge. Hence, regardless of whether there is a laminar or turbulent separation, or reattachment, or shocks, the vorticity input to the viscous layer eventually forms a vortex. The tightness with which this vortex coils and its growth during its passage on the airfoil surface is dependent on various factors, including the state of the boundary layer, and the pressure field set up around the airfoil due to a combination of Mach number and reduced frequency. Nevertheless the stall vortex does form for all conditions studied so far.

3.4. Convection velocity of dynamic stall vortex

Another quantity of interest is the velocity with which the dynamic stall vortex convects over the airfoil. Since the dynamic stall vortex is clearly discernible in the photographs, it was possible to quantify the vortex velocity U_{DSV}, simply by measuring its location for any two consecutive phase angles and dividing the distance travelled by the time difference for the corresponding phase angles. Since the determination of the vortex core is somewhat subjective, scatter is inevitable in the data recovered from the pictures. Despite this limitation, some interesting results emerged from such an analysis and these will be discussed below.

In Fig. 9a through 9d, the convection velocities are plotted as a percentage of the free stream velocity for M = 0.25 to 0.45 at different reduced frequencies. It is very clear from these that regardless of the Mach number or reduced frequency, there exists a plateau at $\frac{U_{DSV}}{U_\infty} = 0.3$ indicating that over most of the airfoil surface, the vortex moves at a constant velocity of $0.3U_\infty$. Three regions can be identified for all cases investigated.

1. A region where the dynamic stall vortex forms and gathers strength.

2. A region where it convects along the surface and grows at the same time.

3. A region, where it grows rapidly and lifts off into the stream.

The character of these three regions depends on the flow parameters, with region 2 becoming broader with increased reduced frequencies. For example, at M = 0.3, for $\kappa = 0.025$, the plateau begins at $\frac{x}{c} = 0.5$; for $\kappa = 0.05$ it begins at 0.4 and for $\kappa = 0.1$ it begins at 0.25. Some where beyond the 75% chord point, the vortex is released into the wake. No clear trends could be observed for this event. Since the amount of vorticity input into the flow near the leading edge is a strong function of the reduced frequency, the above result suggests that the vortex becomes organised 'faster' (i.e. at a station closer to the leading edge) as the frequency increases.

4. Conclusions

1. The dynamic stall vortex is present at all Mach numbers and reduced frequencies. Only its strength appears to differ with Mach number.

2. Increasing the reduced frequency helps in retaining the dynamic stall vortex on the airfoil surface to higher angles of attack, even at the highest Mach numbers tested.

3. Compressibility effects are significant beyond M = 0.3. Dynamic stall occurs at dramatically lower angles of attack as the Mach number exceeds 0.3.

4. The dynamic stall vortex convects at a constant velocity of $0.3\ U_\infty$.

5. The origin of the vortex is NOT clear.

6. No shocks could be seen near the leading edge in the cases studied.

Acknowledgements

This work was initiated by the late Professor Satya Bodapati, who was instrumental in developing the unsteady aerodynamics program in the Navy - NASA Joint Institute of Aeronautics.

The project was funded by ARO-MIPR-137-86 (monitored by Dr. T. Doligalski). Additional support was provided by AFOSR-MIPR-88 (monitored by Capt. H.Helin) and NAVAIR (monitored by Mr. T. Momiyama). The technical support of Mr. Michael J. Fidrich is greatly appreciated.

References

1. Carr, L.W.,"Progress in Analysis and Prediction of Dynamic Stall," *Journal of Aircraft*, Vol. 25,No.1, Jan. 1988, pp 6-17.

2. McCroskey, W.J., "The Phenomenon of Dynamic Stall," NASA TM-81264, March 1981.

3. Lang, J.D., Francis, M.S., "Unsteady Aerodynamics and Dynamic Aircraft Maneuverability," AGARD CP 386. *Unsteady Aerodynamics - Fundamentals and Applications to Aircraft Dynamics*, Goettingen, West Germany, May 6-9, 1985.

4. McCroskey, W.J., McAlister, K.W., Carr, L.W., Pucci, S.L., Lambert, O., and Indergrand, R.F , "Dynamic Stall on Advanced Airfoil Sections," *Journal of American Helicopter Society*, July 1981, pp 45-50.

5. Fung, K.Y., Carr, L.W., "An Analytical Study of Compressibility Effects on Dynamic Stall" *1st National Fluid Mechancis Conference*, Cincinnati, Ohio, July 24 - 28, 1988.

6. Harper, P.W., Flanigan, R.E., "The Effect of Change of Angle of Attack on the Maximum Lift of a Small Model." NACA TN-2061, March 1950

7. Carr, L.W., Chandrasekhara, M.S. "Design and Development of a Compressible Dynamic Stall Facility ", AIAA Paper No. 89-0647, Jan. 1989

8. Reynolds, W.C., Carr, L.W., "Review of Unsteady, Driven , Separated Flows," AIAA Paper No. 85-0527, March 1985.

9. Carr, L.W., McAlister, K.W., McCroskey, W.J., "Analysis of the Development of Dynamic Stall Based on Oscillating Airfoil Experiments," NASA TN D-8382, Jan. 1977.

Table 1: Experimental Conditions

M	κ						
	0	0.0125	0.025	0.05	0.075	0.1	0.15
0.15				X		X	X
0.20	X			X	X	X	
0.25	X	X	X	X	X	X	
0.30	X	X	X	X	X	X	
0.35	X	X	X	X	X	•	
0.40	X		X	X	•	•	
0.45	X		X	X	•	•	

Table 2: Vortex Release Angle of Attack

M	κ					
	0.0125	0.025	0.05	0.075	0.1	0.15
0.15					18.1	19.5
0.20			15.9	17.1	18.3	
0.25	13.8	14.5	15.9	17.1	18.1	
0.30	13.4	14.1	15.9	17.6	18.1	
0.35		13.8	15.2	15.9		
0.40		13.1	14.5			
0.45		12.3	14.2			

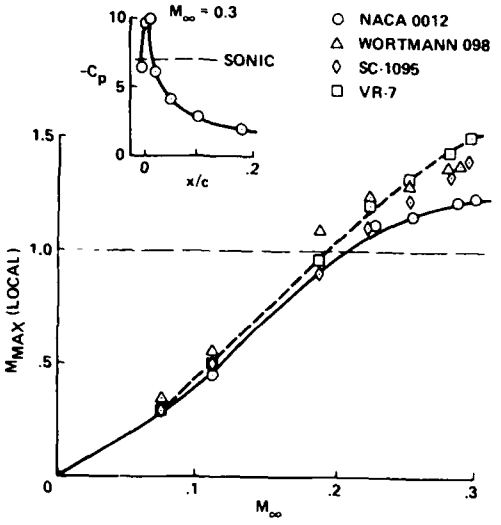

Figure 1. Local Mach Number on Leading Edge of an Oscillating Airfoil vs. Free Stream Mach Number.

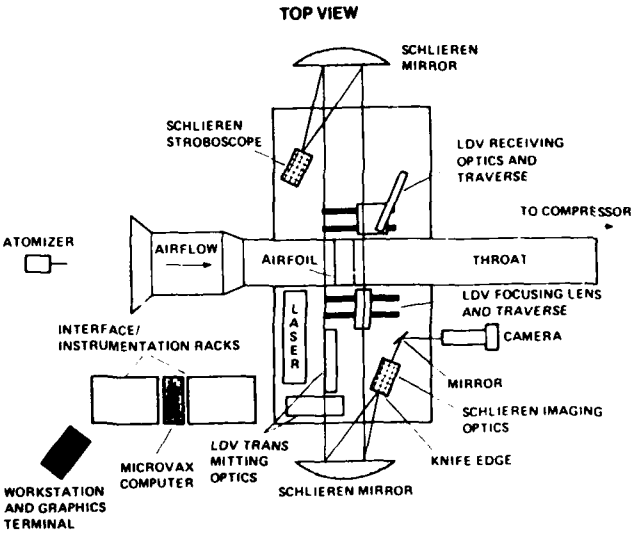

Figure 3. Schematic of the Compressible Dynamic Stall Facility and Instrumentation.

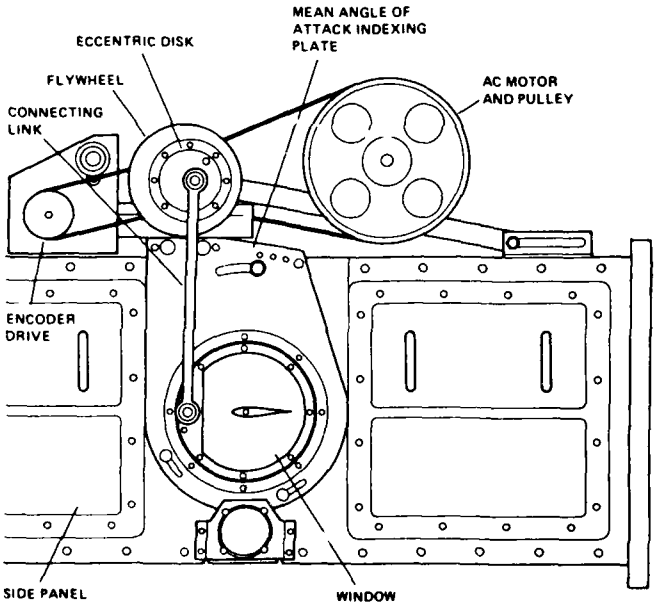

Figure 2. Schematic of the CDSF Test Section.

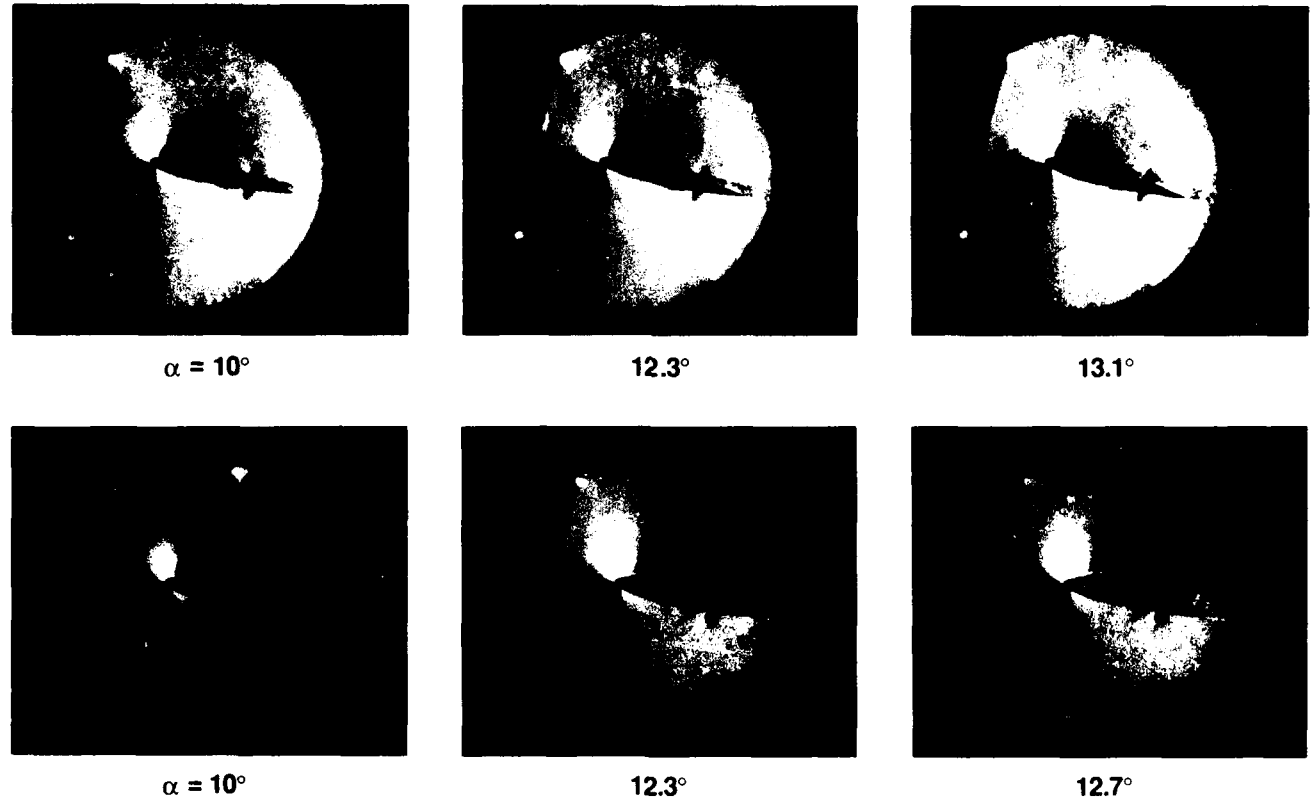

Figure 4. Comparison of the Mach Number Effects on Dynamic Stall Process.
(4a) M = 0.3, κ = 0.05 (4b) M = 0.4, κ = 0.05

(4a)

α = 13.8° 14.5° 15.2°

(4b)

α = 13.8° 14.5° 15.2°

Figure 4 (cont'd)

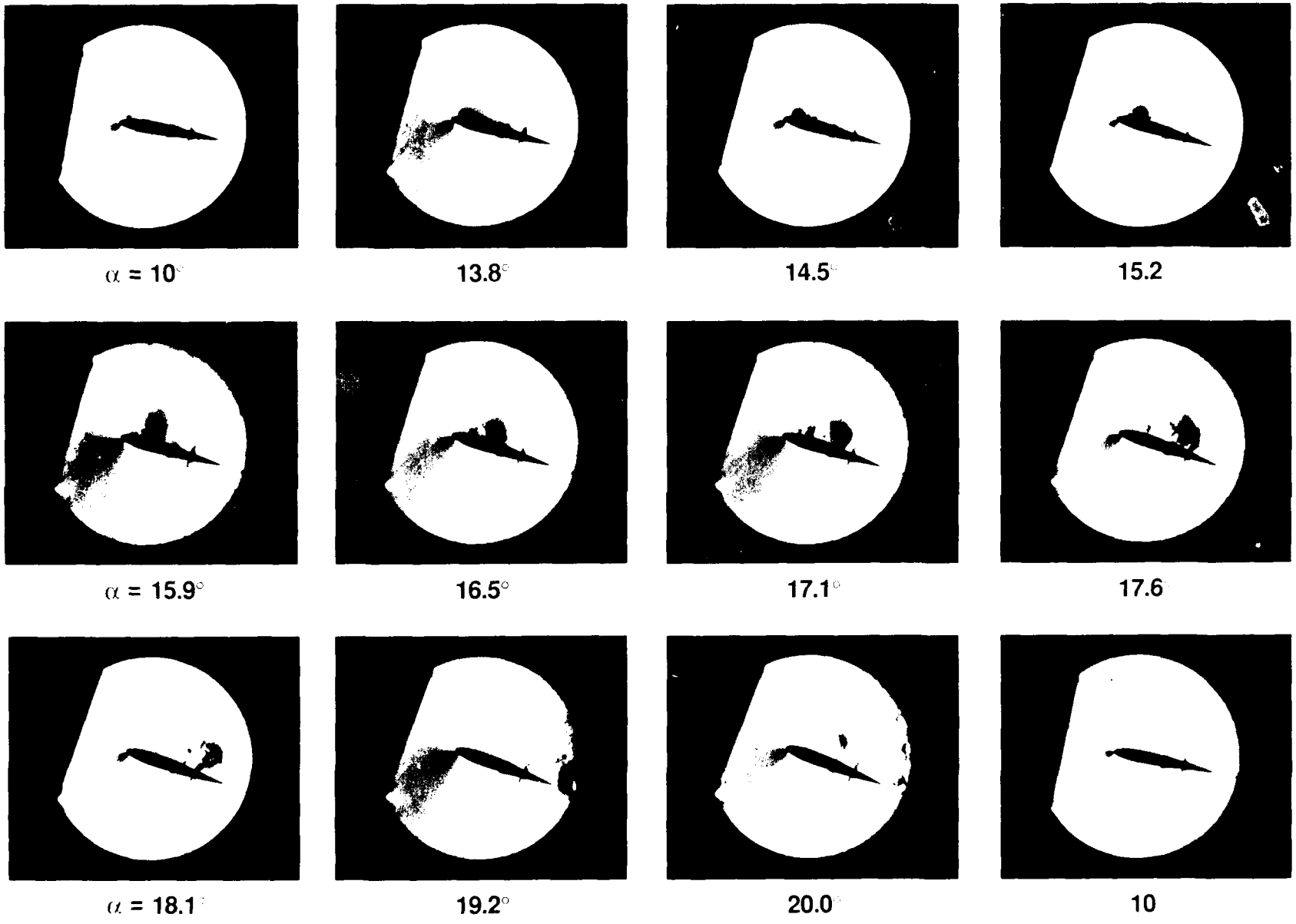

Figure 5a. Stroboscopic Schlieren Photographs of the Compressibility Effects on Dynamic Stall of an Oscillating Airfoil: M = 0.2, $\kappa = 0.1$, $\alpha = 10° + 10° \sin \omega t$.

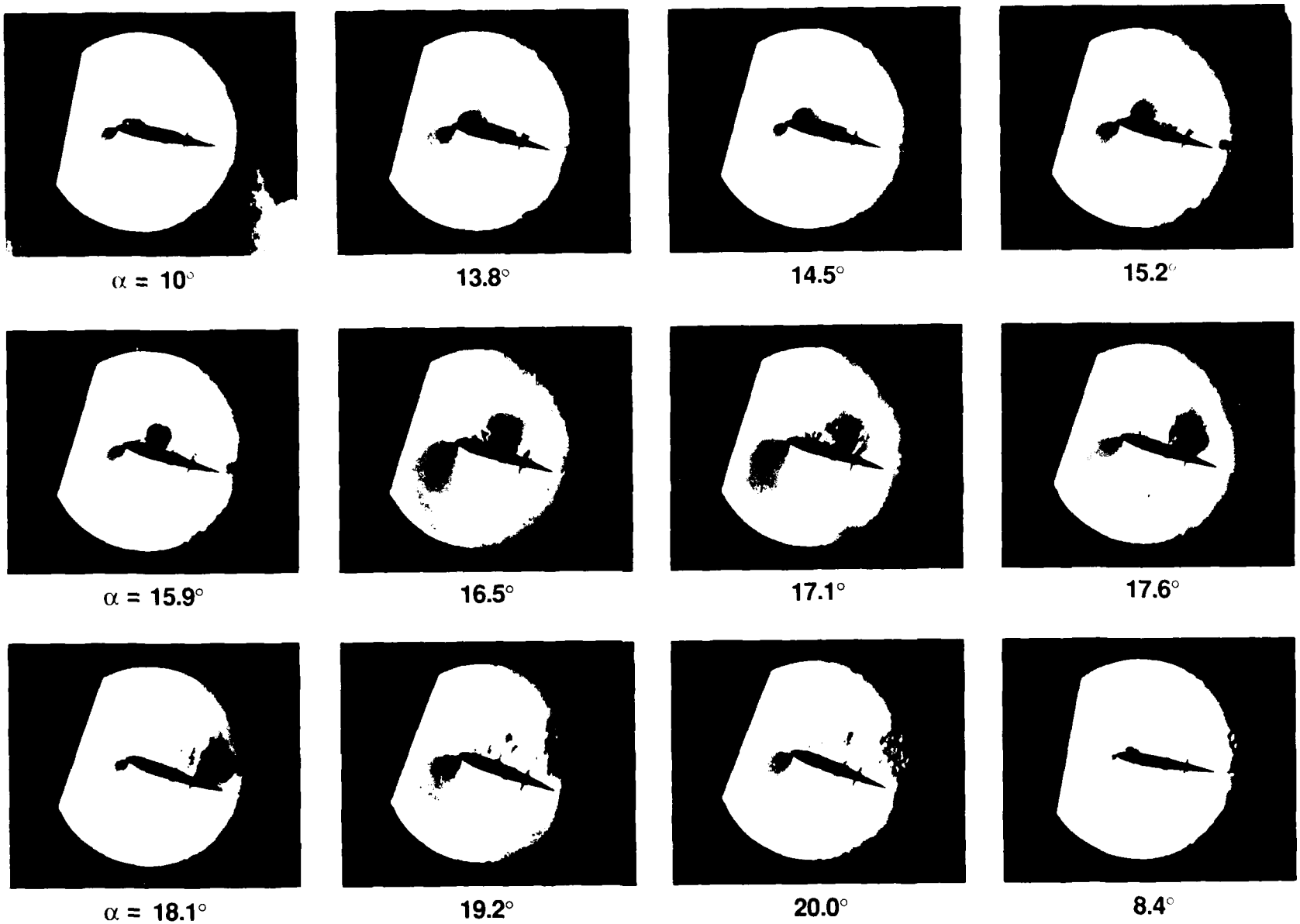

Figure 5b. Stroboscopic Schlieren Photographs of the Compressibility Effects on Dynamic Stall of an Oscillating Airfoil: $M = 0.3$, $\kappa = 0.1$, $\alpha = 10° + 10° \sin \omega t$.

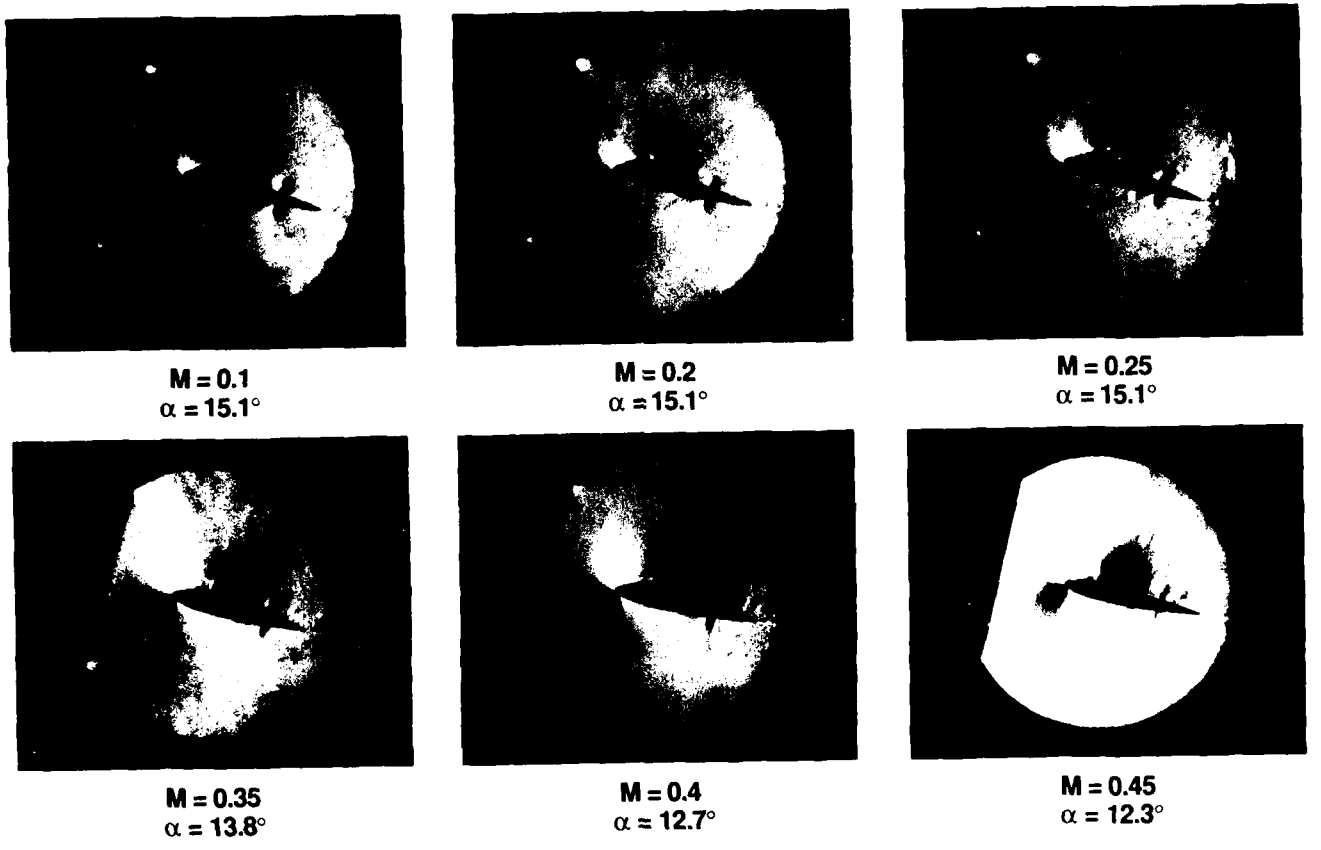

Figure 6. **Effects of Compressibility on Dynamic Stall of an Oscillating Airfoil: Schlieren Studies; $\kappa = 0.05$.**

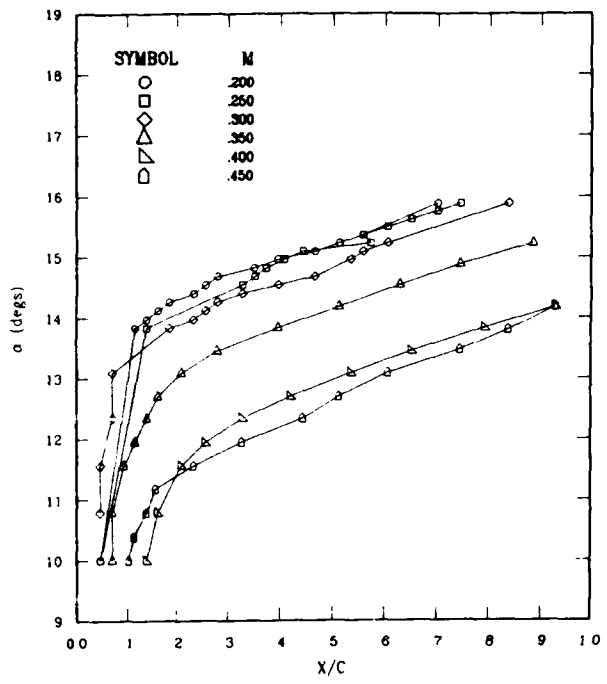

Figure 7. Quantitative Effects of Mach Number on Dynamic Stall Process, $\kappa = 0.05$.

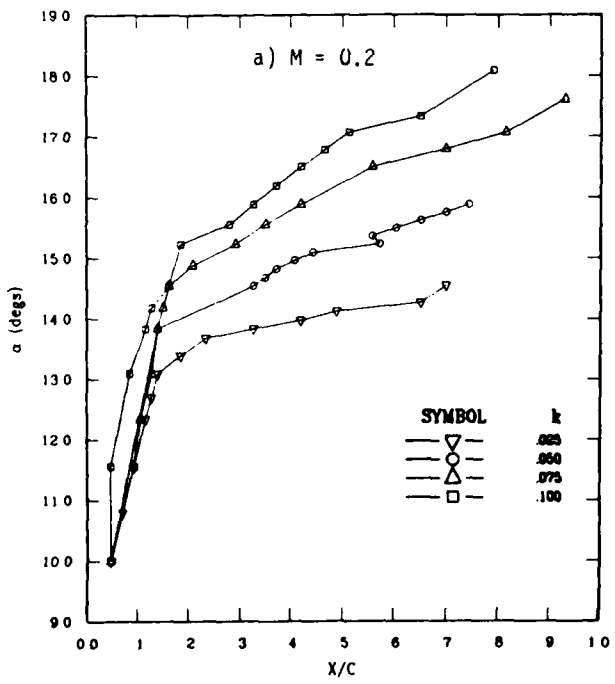

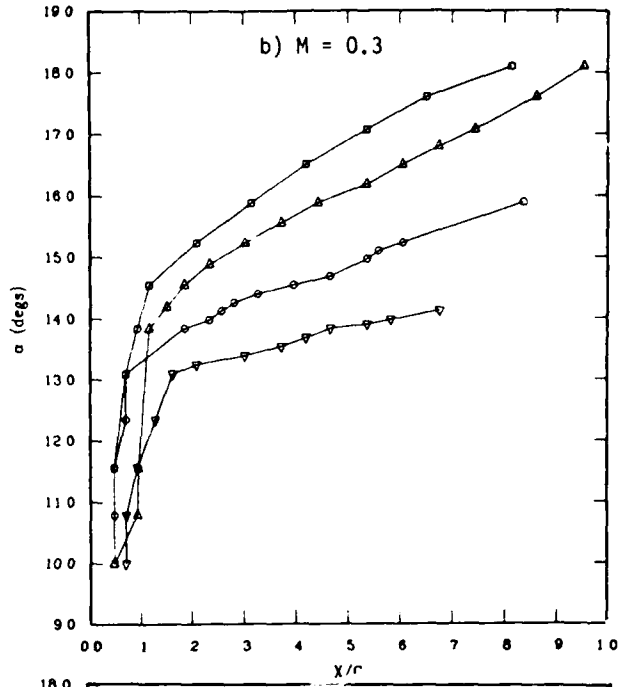

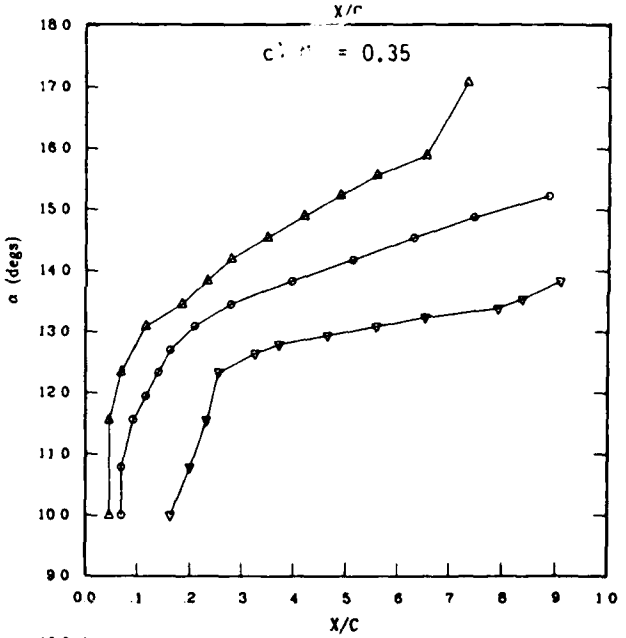

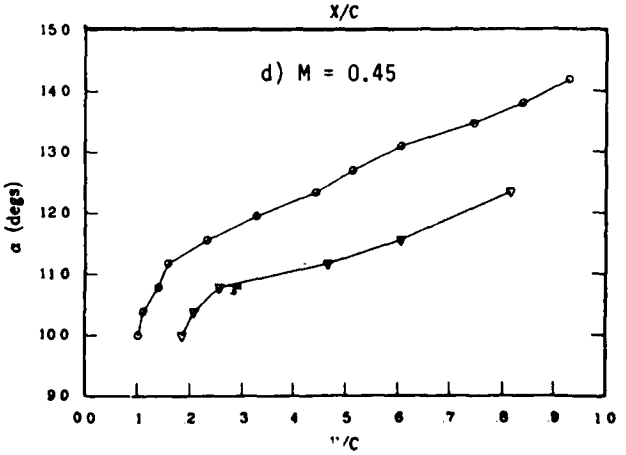

Figure 8. Effects of Reduced Frequency on Dynamic Stall. a) M = 0.2, b) M = 0.3, c) M = 0.35, d) M = 0.45.

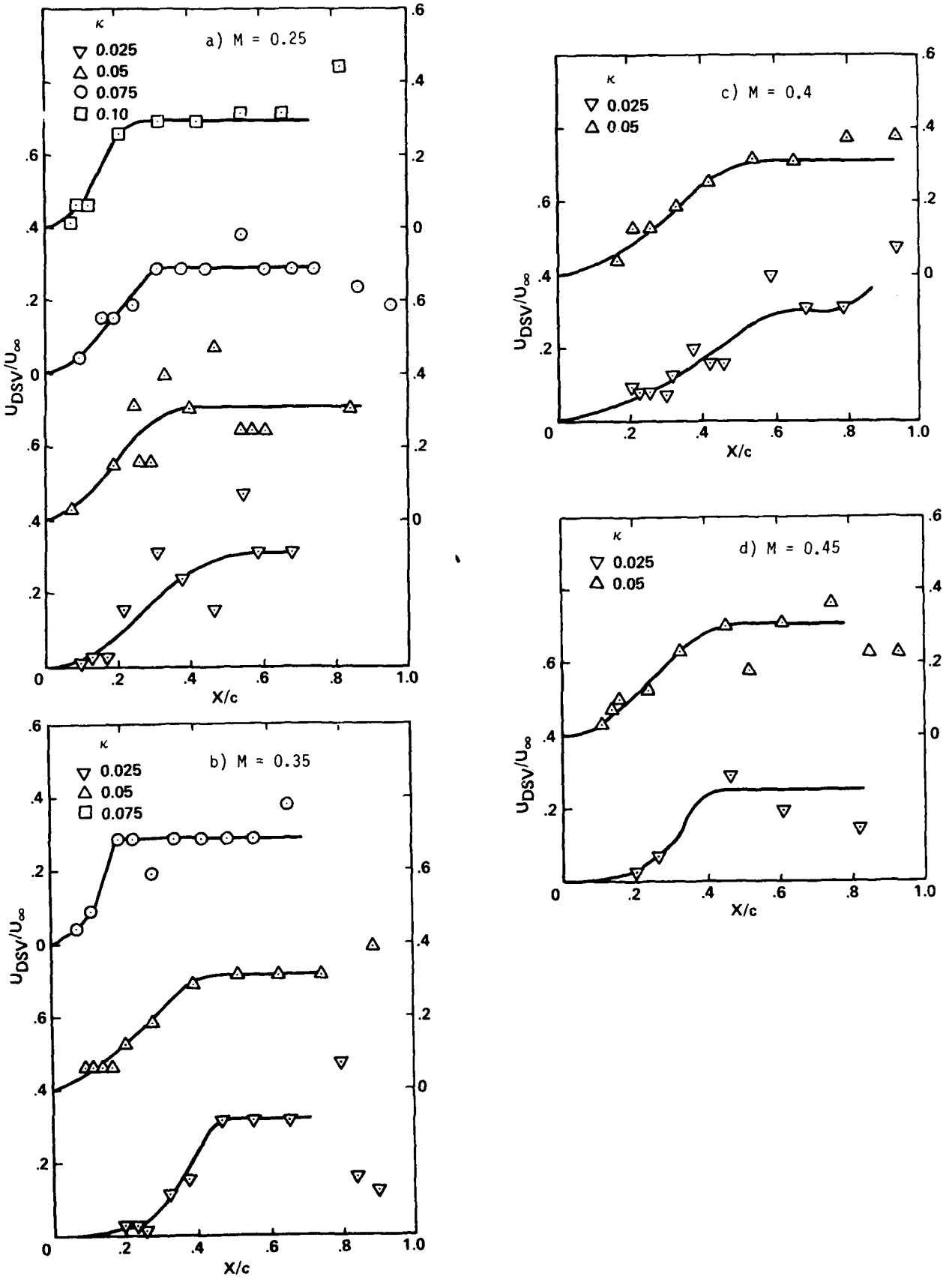

Figure 9. Convection Velocity of the Dynamic Stall Vortex. a) M = 0.25, b) M = 0.35, c) M = 0.4, d) M = 0.45.